

# Intrinsic Nucleic Acid-Binding Activity of Chp1 Chromodomain Is Required for Heterochromatic Gene Silencing

Mayumi Ishida,<sup>1,2</sup> Hideaki Shimojo,<sup>3</sup> Aki Hayashi,<sup>1</sup> Rika Kawaguchi,<sup>1</sup> Yasuko Ohtani,<sup>1</sup> Koichi Uegaki,<sup>4</sup> Yoshifumi Nishimura,<sup>3,\*</sup> and Jun-ichi Nakayama<sup>1,2,5,\*</sup>

<sup>1</sup>Laboratory for Chromatin Dynamics, RIKEN Center for Developmental Biology, Kobe, Hyogo 650-0047, Japan

<sup>2</sup>Department of Bioscience, Graduate School of Science and Technology, Kansai University, 2-1 Gakuen, Suita, Hyogo 669-1337, Japan

<sup>3</sup>Graduate School of Supramolecular Biology, Yokohama City University, 1-7-29, Suehiro-cho, Tsurumi-ku, Yokohama 230-0045, Japan

<sup>4</sup>National Institute of Advanced Industrial Science and Technology, 1-8-31 Midorigaoka, Ikeda, Osaka 563-8577, Japan

<sup>5</sup>Graduate School of Natural Sciences, Nagoya City University, Nagoya 467-8501, Japan

\*Correspondence: jnakayam@cdb.riken.jp (J.-i.N.), nisimura@tsurumi.yokohama-cu.ac.jp (Y.N.)

DOI 10.1016/j.molcel.2012.05.017

## SUMMARY

Centromeric heterochromatin assembly in fission yeast requires the RNAi pathway. Chp1, a chromodomain (CD) protein, forms the Ago1-containing RNA-induced transcriptional silencing (RITS) complex and recruits siRNA-bound RITS to methylated histone H3 lysine 9 (H3K9me) via its CD. Here, we show that the CD of Chp1 (Chp1-CD) possesses unique nucleic acid-binding activities that are essential for heterochromatic gene silencing. Detailed electrophoretic-mobility shift analyses demonstrated that Chp1 binds to RNA via the CD in addition to its central RNA-recognition motif. Interestingly, robust RNA- and DNA-binding activity of Chp1-CD was strongly enhanced when it was bound to H3K9me, which was revealed to involve a positively charged domain within the Chp1-CD by structural analyses. These results demonstrate a role for the CD that provides a link between RNA, DNA, and methylated histone tails to ensure heterochromatic gene silencing.

## INTRODUCTION

In eukaryotic cells, the formation of higher-order chromatin structure, called heterochromatin, plays an important role in diverse chromosomal processes. Heterochromatin is generally transcriptionally silent, and the assembly of silent chromatin is intimately linked with changes in posttranslational histone tail modifications. The methylation of histone H3 lysine 9 (H3K9me) by SUV39H family methyltransferases, which is a hallmark of heterochromatin, acts as a binding site for a set of chromatin proteins that includes the evolutionarily conserved heterochromatin protein 1 (HP1) (Bannister et al., 2001; Lachner et al., 2001; Nakayama et al., 2001).

In the fission yeast *Schizosaccharomyces pombe*, heterochromatin is essential for forming functional chromosomal domains

such as centromeres, the mating-type region, and telomeres (Allshire et al., 1995; Grewal and Jia, 2007). Fission yeast heterochromatin is characterized by H3K9 methylation by Ctr4, a homolog of mammalian SUV39H. This methylation provides docking sites for two HP1 proteins, Swi6 and Chp2 (Bannister et al., 2001; Nakayama et al., 2001; Sadaie et al., 2004), which, in turn, recruit a wide range of chromatin proteins to form repressive chromatin structures (Fischer et al., 2009; Motamedi et al., 2008; Sadaie et al., 2008). The assembly and maintenance of centromeric heterochromatin is directly linked to the RNA interference (RNAi) pathway (Bühler and Moazed, 2007; Grewal and Jia, 2007). Centromeric DNA repeats are weakly transcribed in the G1/S phase (Chen et al., 2008; Kloc et al., 2008), and the processing of these transcripts through the RNAi pathway is coupled with the targeting of Ctr4 methyltransferase activity to the centromeric regions (Volpe et al., 2002).

In currently proposed models, siRNAs are loaded onto the argonaute protein Ago1, a component of the RNA-induced transcriptional silencing (RITS) complex, which also contains the chromodomain protein Chp1 and the GW-repeat protein Tas3 (Verdel et al., 2004). The RITS complex targets nascent centromeric transcripts through base-pairing interactions with Ago1-bound siRNAs and by Chp1's association with H3K9me (Bühler et al., 2006; Partridge et al., 2002). This interaction leads to the recruitment of RNA-dependent RNA polymerase complex (RDRC), which contains the RNA-dependent RNA polymerase Rdp1, the RNA helicase Hrr1, and the polyA polymerase-family protein Cid12 (Motamedi et al., 2004). The RDRC then synthesizes double-stranded RNAs (dsRNAs) that are processed into siRNAs by Dicer (Dcr1) and are transported to the RITS complex (Buker et al., 2007; Motamedi et al., 2004; Sugiyama et al., 2005). Chromatin-associated RITS also recruits the Ctr4 complex (CLRC) to methylate H3K9. Deleting any of the RNAi components causes the loss of centromeric silencing and reduces H3K9me and Swi6 recruitment (Volpe et al., 2002), while deleting Ctr4 impairs siRNA production and heterochromatin formation (Motamedi et al., 2004; Noma et al., 2004; Sadaie et al., 2004; Shanker et al., 2010). Therefore, it is thought that centromeric heterochromatin is maintained by a self-enforcing loop involving H3K9me and the RNAi pathway.

The chromodomain (CD) is an evolutionarily conserved protein module that was first identified in the *Drosophila* proteins HP1 and Polycomb (Pc) (Paro and Hogness, 1991). The CD's best-recognized target is the methylated histone tail: HP1's CD binds to H3K9me (Bannister et al., 2001; Lachner et al., 2001; Nakayama et al., 2001), and Pc's CD binds to K27-methylated histone H3 (Bernstein et al., 2006). Several lines of evidence suggest that the CD, in addition to targeting methylated histones, also binds to DNA and RNA (Akhtar et al., 2000; Bouazoune et al., 2002). For example, two components of *Drosophila* dosage-compensation complex, MOF and MSL3, contain a CD that binds to RNA (Akhtar et al., 2000). A mouse Pc homolog, Cbx7, can also bind to RNA (Bernstein et al., 2006); the noncoding RNA *ANRIL* was suggested to be one of its *in vivo* targets (Yap et al., 2010). The CD in the *S. cerevisiae* Esa1 histone acetyltransferase also binds to RNA (Shimojo et al., 2008). Although both the RNA-binding and methylated histone-binding activities of CDs are known to be important for CD protein functions in several biological processes, the physical and functional relationships between these two activities are poorly understood.

In *S. pombe*, four CD proteins, Clr4, Chp1, Chp2, and Swi6, have confirmed functional roles in heterochromatin assembly. Since these proteins use and share the same H3K9me marks to bind to target chromatin, it is important to understand the mechanism by which they recognize H3K9me and how their distinct functions are coordinated at the same locus. Chp2's CD (Chp2-CD) and Swi6's CD (Swi6-CD) have comparable H3K9me-binding affinities (Sadaie et al., 2008), whereas Clr4's CD (Clr4-CD) binds to H3K9me with a slightly higher affinity than Swi6-CD (Zhang et al., 2008). Chp1-CD's H3K9me-binding affinity, which is critical for establishing heterochromatin, is the highest among these four CDs (Schalch et al., 2009). Chp1 targets H3K9me-enriched chromatin via its N-terminal CD (Noma et al., 2004; Partridge et al., 2002; Sadaie et al., 2004; Verdel et al., 2004) and recruits the RITS complex through interaction between its C-terminal region and Tas3 (Partridge et al., 2007). While Chp1 possesses a putative RNA recognition motif (RRM) in its central region, the RRM's RNA-binding activity and functional importance have remained obscure (Petrie et al., 2005).

Here, we demonstrate that Chp1 binds to RNA via both its N-terminal CD and its central RRM. The CD of Chp1, however, shows robust RNA- and DNA-binding activity when it is bound to H3K9me. Structural and mutational analyses revealed that Chp1 uses a positively charged domain for this induced activity. *In vivo* analyses confirmed that these nucleic acid-binding activities contribute to Chp1's silencing function. Interestingly, a similar nucleic acid-binding ability was also associated with Clr4's CD (Clr4-CD) when bound to H3K9me. These nucleic acid-binding activities appeared to provide a division of roles and set an order of chromatin targeting among four CD proteins in the formation of higher-order chromatin structure.

## RESULTS

### Chp1 Binds to Single-Stranded RNA via Two Distinct Domains

To investigate the possibility that Chp1 function involves an RNA-binding activity, we first conducted an electrophoretic-

mobility shift assay (EMSA) using an *in vitro* transcribed centromeric RNA (*cen* RNA) as a probe to investigate whether Chp1 directly binds to RNA. A centromeric repeat region (376 bp) previously characterized as small RNA-generating clusters (Djupedal et al., 2009) was cloned and used for *in vitro* transcription. The full-length Chp1 and GST-fusions of three truncated fragments (Chp1-1/3, Chp1-2/3, and Chp1-3/3) were expressed and affinity-purified for the EMSA (Figures 1A and 1B). GST alone was used as a negative control.

In this assay, the full-length Chp1 showed a robust RNA-binding activity (Figure 1C). Chp1 possesses a putative RRM in its central region (Petrie et al., 2005), and the central Chp1-2/3 fragment that contained this RRM showed similar RNA-binding activity (Figure 1C). Interestingly, the N-terminal Chp1-1/3 fragment in which the CD was located also bound to centromeric (*cen*) RNA, but the C-terminal Chp1-3/3 fragment did not. Since previous reports suggest that several CDs can bind to RNA (Akhtar et al., 2000; Bernstein et al., 2006; Shimojo et al., 2008), the conserved Chp1-CD region (residues 20–75) was expressed as a GST-fusion protein (GST-Chp1-CD) (Figure 1B) and examined by RNA EMSAs. This conserved CD fragment was also able to bind to the *cen* RNA (Figure 1C). In contrast, a Chp1-1/3 construct lacking the Chp1-CD central region failed to retain the *cen* RNA-binding activity (Figures 1D and 1E, Chp1-1/3- $\Delta$ 38–55), indicating that Chp1-1/3's RNA binding was likely mediated by the CD. Within the Chp1-2/3 fragment, a central 312–407 region corresponding to the putative RRM was confirmed to be responsible and required for the RNA binding observed for this fragment (Figures S1A and S1B). These results suggested that Chp1 binds to single-stranded RNA via at least two distinct domains, the N-terminal CD and the central RRM.

### Among Four H3K9me-Recognizing *S. pombe* CDs, Only Chp1-CD Shows RNA-Binding Activity

The assembly of fission yeast heterochromatin requires three CD proteins in addition to Chp1, namely, H3K9 methyltransferase Clr4 and the HP1 proteins Swi6 and Chp2 (Figure 1F). To determine whether CDs other than Chp1-CD can also bind RNA, the CD region of each of these proteins was produced as a GST-fusion protein and subjected to the EMSA (Figures 1G and 1H). Chp1-CD clearly bound *cen* RNA, but the other CDs did not. This result suggested that the RNA-binding activity is associated with only a subset of CDs, and that this RNA binding is linked specifically with Chp1 function in RNAi-directed heterochromatin assembly. Due to this observed unique function of the Chp1-CD, the biological importance of its RNA-binding activity was investigated in further detail.

### Chp1-CD Binds to RNA without Any Particular Sequence Specificity

It has been proposed that centromeric transcripts fold in part into a double-stranded secondary structure (Djupedal et al., 2009). To gain insight into the type of sequences that are targeted by Chp1-CD's RNA-binding activity, we prepared a series of truncated RNAs differing in length and position within the original *cen* RNA (Figure S1C) and subjected them to the RNA EMSA. Although Chp1-CD showed a slightly higher affinity for longer transcripts, it was able to bind all the *in vitro*-transcribed RNAs ranging in

Molecular Cell

Chp1 CD links RNA and K9-Methylated Histone H3

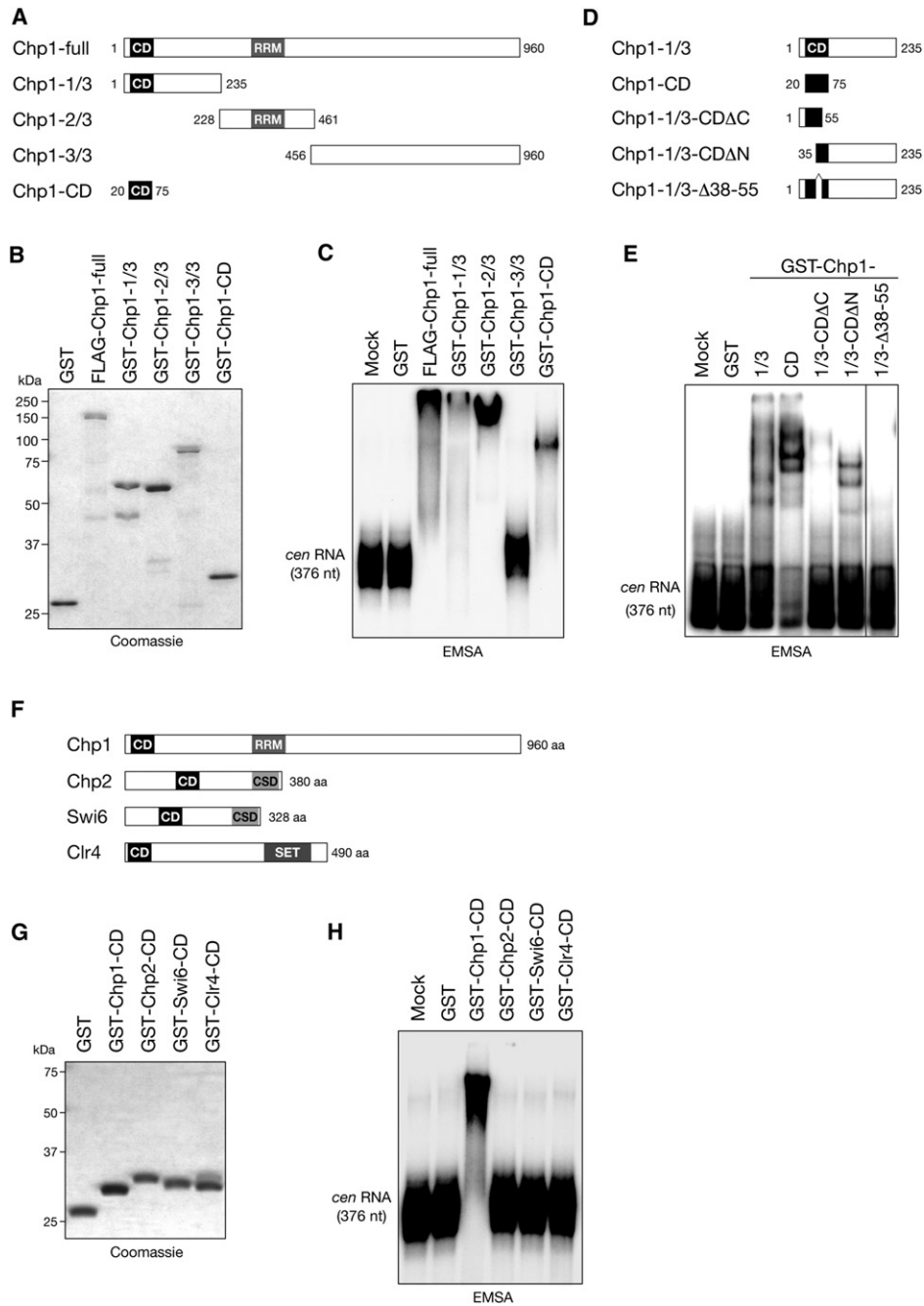


**Figure 1. The Chp1 Chromodomain Binds RNA**

(A) Schematic of recombinant Chp1 proteins used in the electrophoretic-mobility shift assay (EMSA): full-length Chp1 (Chp1-full); truncated Chp1 containing the N-terminus (Chp1-1/3), middle part (Chp1-2/3), or C terminus (Chp1-3/3); and Chp1 chromodomain (Chp1-CD). The chromodomain (CD) and a putative RNA recognition motif (RRM) are indicated by black and gray boxes, respectively.

(B) Recombinant proteins used in (C) were resolved by 17% SDS-PAGE and visualized by Coomassie staining.

(C) EMSA using FLAG-tagged, full-length Chp1 (FLAG-Chp1-full) and GST-fused recombinant proteins. A <sup>32</sup>P-labeled, 376 nt single-stranded RNA corresponding to the centromeric *dh* repeat was used as probe. Mock: a reaction lacking recombinant proteins. GST alone was used as a negative control.

(D) Schematic of the truncated recombinant Chp1 proteins used in (E).

(E) EMSA using GST-fused truncated Chp1 proteins or GST alone.

(F) Schematic of four chromodomain proteins: Chp1, Chp2, Swi6, and Clr4. Black and light gray boxes in Chp2 and Swi6 represent the conserved chromodomain (CD) and the chromoshadow domain (CSD), respectively. A dark gray box in Clr4 represents the SET domain.

(G) Proteins used in (H).

(H) EMSA using GST-fused recombinant CDs of Chp1, Chp2, Swi6, and Clr4 or of GST alone.

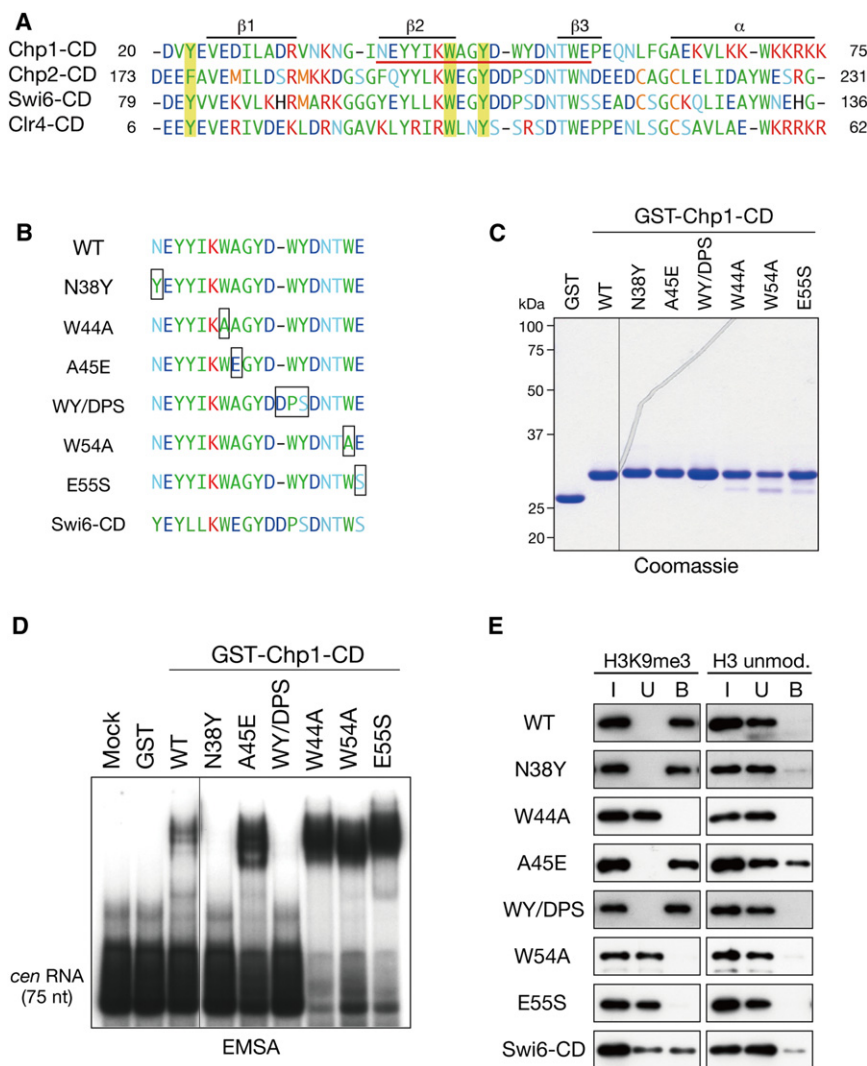


**Figure 2. Identification of Residues Required for Chp1-CD to Bind RNA**

(A) Chromodomain alignment of Chp1, Chp2, Swi6, and Clr4. Three yellow boxes indicate residues that form aromatic pockets that recognize K9 methylated histone H3 (Jacobs and Khorasanizadeh, 2002). Amino acids are represented by colors indicating the chemical nature of the side chain: negatively charged and hydrophilic (blue), positively charged and hydrophilic (red), polar and hydrophilic (sky blue), hydrophobic (green), or sulfur-containing (orange). The positions of secondary structure elements are indicated above the alignment.

(B) Alignment of wild-type and mutant Chp1-CDs (38-55 aa) with the Swi6-CD (98-116 aa). Boxes indicate substituted amino acids.

(C) GST-fused recombinant proteins used in (D) and (E).

(D) EMSA using wild-type and mutant Chp1-CDs; a <sup>32</sup>P-labeled, 75-nt single-stranded RNA for centromeric *dh* repeat was used as a probe.

(E) Peptide pull-down assays using wild-type or mutant Chp1-CD or Swi6-CD. Input (I), unbound (U), and bound (B) fractions were analyzed by western blot using  $\alpha$ GST antibodies.

length from 75 to 376 nt (Figure S1D and data not shown). In addition, Chp1-CD bound to single-strand RNAs corresponding to the *ura4<sup>+</sup>* transcript and antisense RNAs of the original *cen* RNA (Figure S1E and data not shown). Although we could not rule out the possibility that Chp1-CD recognizes partially structured RNAs, these results suggested that Chp1-CD binds to RNA without any preference for particular structures or sequences.

To investigate whether Chp1-CD could also bind to DNA, we next examined single-stranded (ssDNA) and double-stranded DNA (dsDNA) corresponding to centromeric repeats. While Chp1-1/3 and Chp1-2/3 were able to bind both ssDNA and dsDNA, the Chp1-CD fragment did not bind to ssDNA and bound only negligibly to dsDNA (Figure S1F). These results suggested that Chp1-CD preferentially binds single-stranded RNA transcripts.

#### Residues Involved in Chp1-CD's RNA Binding Are Distinct from Those Required for H3K9me Recognition

To understand the biological implications of Chp1-CD's RNA binding, the CD residues essential for the RNA-binding activity

were next investigated using a 75 nt portion of the *cen* RNA. Amino acid substitutions were introduced into an internal core region of the Chp1-CD that was required for its ability to bind RNA (Figure 1E; underlined in red in Figure 2A). The Swi6-CD does not bind RNA (Figure 1H), and thus Chp1-CD residues were substituted with the corresponding sequence in Swi6-CD (Figure 2B; N38Y, A45E, WY/DPS, and E55S). A further two Chp1-CD mutants contained Ala substitutions at the highly conserved W44A and W54A (Figure 2B). W44 is one of three hydrophobic residues required for recognizing K9-methylated histone H3 (Figure 2A) (Jacobs and Khorasanizadeh, 2002). An EMSA demonstrated that the two Chp1-CD mutants with N38Y and WY/DPS lost the ability to bind RNA (Figure 2D), indicating that residues N38, W49, and Y50 are critical for Chp1-CD to bind RNA. In contrast, other Chp1-CD mutants bound to *cen* RNA with somewhat higher affinities than shown by wild-type (WT) Chp1-CD (Figure 2D).

To further investigate the relationship between Chp1-CD's H3K9me and RNA binding, we conducted a peptide pull-down assay to test the mutated CD's ability to bind to H3K9me (Figure 2E). In this assay, wild-type Chp1-CD bound strongly to H3K9me3 peptide but only negligibly to unmodified H3 peptides (Figure 2E, WT). Consistent with a previous report (Schalch et al., 2009), Swi6-CD's binding to H3K9me3 peptide was weaker than that of Chp1-CD. The altered Chp1-CDs that lost RNA-binding ability (N38Y and WY/DPS) were found to still retain the H3K9me peptide-binding activity similar to that of WT (Figure 2E). This was confirmed by isothermal titration calorimetry (ITC) that

## Molecular Cell

### Chp1 CD links RNA and K9-Methylated Histone H3

showed Chp1-CD-N38Y and Chp1-CD-WY/DPS had H3K9me3-binding affinities comparable to that of Chp1-CD-WT (Figures S2A–S2C and S2G). In contrast, the three other mutants W44A, W54A, and E55S that all had strong RNA-binding activity (Figure 2D) were not able to bind H3K9me3 (Figures 2E and S2D). These results suggested that residues involved in Chp1-CD's RNA binding are distinct from those required for H3K9me recognition.

#### H3K9me Enhances Chp1-CD RNA- and DNA-Binding Activity

To determine whether Chp1-CD binds simultaneously to RNA and H3K9me, unmodified H3 or H3K9me2 peptide were next included in the EMSA (Figure 3). In this assay, the H3K9me2 was used because it is a preferential heterochromatin mark *in vivo*. The addition of H3K9me2 peptide, but not of unmodified H3 peptide, led to a supershift of the original band formed by *cen* RNA and Chp1-CD-WT (Figure 3A). This supershift was not observed in the assay using H3K9me-binding-deficient Chp1-CD-W44A (Figure 3B), suggesting that Chp1-CD was able to form a ternary complex with H3K9me and RNA. The addition of unmodified H3 peptide appeared to exert a negative effect on Chp1-CD RNA binding (Figure 3A). Since Chp1-CD did not bind to unmodified H3 peptide (Figure 2E), this was likely due to an electrostatic interaction between unmodified H3 peptide and the RNA probe that inhibited the ability of Chp1-CD-WT to bind to probe.

Intriguingly, the addition of H3K9me2 peptide appeared to enhance Chp1-CD-WT binding of RNA (Figure 3A, see free *cen* RNA probe). Furthermore, two mutants without RNA-binding activity, N38Y and WY/DPS (Figure 2D), acquired the ability to bind RNA when H3K9me2 peptide was present (Figures 3C and S3A). These results suggested that while free Chp1-CD is able to bind RNA, additional interaction with H3K9me changes its RNA-binding properties.

Chp1-CD RNA-binding activity was further examined by titration EMSA analyses (Figures 3E, 3F, S3B, and S3C). Free Chp1-CD bound RNA with an affinity of  $K_D = 3.85 \pm 0.33 \mu\text{M}$ , which was slightly weaker than that of the Chp1-2/3 containing RRM ( $K_D = 1.97 \pm 0.02 \mu\text{M}$ ). Notably, H3K9me2-bound Chp1-CD showed nearly ten times stronger affinity ( $K_D = 0.37 \pm 0.01 \mu\text{M}$ ) (Figures 3E, 3F, and S3C). Unexpectedly, H3K9me2-bound Chp1-CD also showed strong affinity for ssDNA and dsDNA (Figure 3D). Titration analyses revealed that the binding affinity for dsDNA was almost comparable to that for RNA ( $K_D = 0.37 \pm 0.02 \mu\text{M}$ ) (Figures 3E, 3F, and S3C). These results suggested that Chp1-CD could interact with both RNA and DNA when bound to H3K9me, and imply that this induced activity contributes to stable chromatin binding of Chp1 in establishing centromeric heterochromatin. It seems likely that free Chp1-CD changes its structure upon binding to H3K9me in a manner that offers additional interfaces for interacting with RNA and DNA.

#### Basic Residues in Chp1-CD's C-Terminal $\alpha$ -Helix Are Involved in the Induced RNA- and DNA-Binding

To investigate how Chp1-CD binds to RNA and DNA,  $^{15}\text{N}$ -labeled and  $^{15}\text{N}$ ,  $^{13}\text{C}$ -labeled Chp1-CDs (residues 1–75) were produced and monitored by conventional multidimensional

NMR methods (Figures S4A and S4B). While W49 and Y50 were determined to be critical for free Chp1-CD to bind RNA (Figure 2D), the corresponding region (G46–N52) could not be assigned in the NMR analysis (Figure S4C), probably due to its structural flexibility. In addition, only a weak chemical shift was observed for N38 when *cen* RNA was present (Figure S4C). It is possible that N38 may indirectly affect the RNA binding of free Chp1-CD.

To gain further insight into the mechanisms underlying Chp1-CD's binding of RNA and DNA, we next examined its solution structure in complex with H3K9me3 peptide (residues 1–18) (Figures 4A and S4E–S4G and Table 1). The overall architecture of Chp1-CD determined by this NMR analysis in the absence of RNA could be superimposed on the previously determined crystal structure of Chp1-CD (residues 9–76) bound to H3K9me3 peptide (residues 1–16) (Schalch et al., 2009). The root-mean-square-deviations (RMSDs) of the backbone heavy atoms between NMR and crystal structure were 1.60 Å for 19–73 amino acids and 0.69 Å for 20–32, 38–44, and 52–73 amino acids. The NMR analysis also revealed the presence of a small  $3^{10}$  helix formed by residues 17–20 (Figure 4A). Adding 75 nt *cen* RNA led to a chemical shift of amide protons for residues within both this  $3^{10}$  helix and in a C-terminal  $\alpha$ -helix composed of residues 62–75 (Figures 4A, indicated in red, and S4B and S4D). The N-terminal  $3^{10}$  helix contributes to form an acidic surface, whereas the C-terminal  $\alpha$ -helix contains a stretch of basic amino acid residues and forms a positively charged surface with the N-terminal residues of the bound H3K9me peptide (Figure 4B). This positively charged surface appeared unique to Chp1; no such charged domain was found for free Swi6-CD determined by NMR analysis (Figure 4C).

Amino acid substitutions were next introduced within the positively charged C-terminal  $\alpha$ -helix surface to examine whether it was involved in the RNA binding by Chp1-CD complexed with H3K9me (Figure 4D and 4E). To maintain the overall Chp1-CD structure, conserved hydrophobic residues (V66, L67, and W70) were not changed, and only basic residues were replaced with residues corresponding to those in Swi6-CD (Figure 4D,  $\alpha\text{mut1}$  and  $\alpha\text{mut2}$ ). The same amino acid substitutions were also introduced into the Chp1-CD-N38Y and Chp1-CD-WY/DPS constructs, which were able to bind RNA when H3K9me2 was present (Figures 3C and S3A). As shown in Figures 3 and S3A, Chp1-CD-WT, Chp1-CD-N38Y, and Chp1-CD-WY/DPS bound to RNA in the presence of H3K9me2 peptides (Figure 4F). Notably, however, the addition of either the  $\alpha\text{mut1}$  or  $\alpha\text{mut2}$  mutation to these CDs completely abolished their RNA-binding activity (Figure 4F). The effect of  $\alpha\text{mut2}$  was almost the same as that of  $\alpha\text{mut1}$ , indicating that the distal five residues (K71–K75) play an essential role in the H3K9me-bound Chp1-CD's binding of RNA. Mutant Chp1-CD with  $\alpha\text{mut1}$  also failed to bind ssDNA or dsDNA even in the presence of H3K9me2 peptide (data not shown). These results suggested that the C-terminal  $\alpha$ -helix was involved in the induced RNA- and DNA-binding activity of Chp1-CD. It was unlikely that impaired RNA- and DNA-binding activity of Chp1-CD was simply due to C-terminal  $\alpha$ -helix mutations severely affecting H3K9me binding, since Chp1-CD containing  $\alpha\text{mut1}$  or  $\alpha\text{mut2}$  was able to bind to H3K9me3 with an affinity comparable to that of Chp1-CD-WT (Figures 4G and S2E).

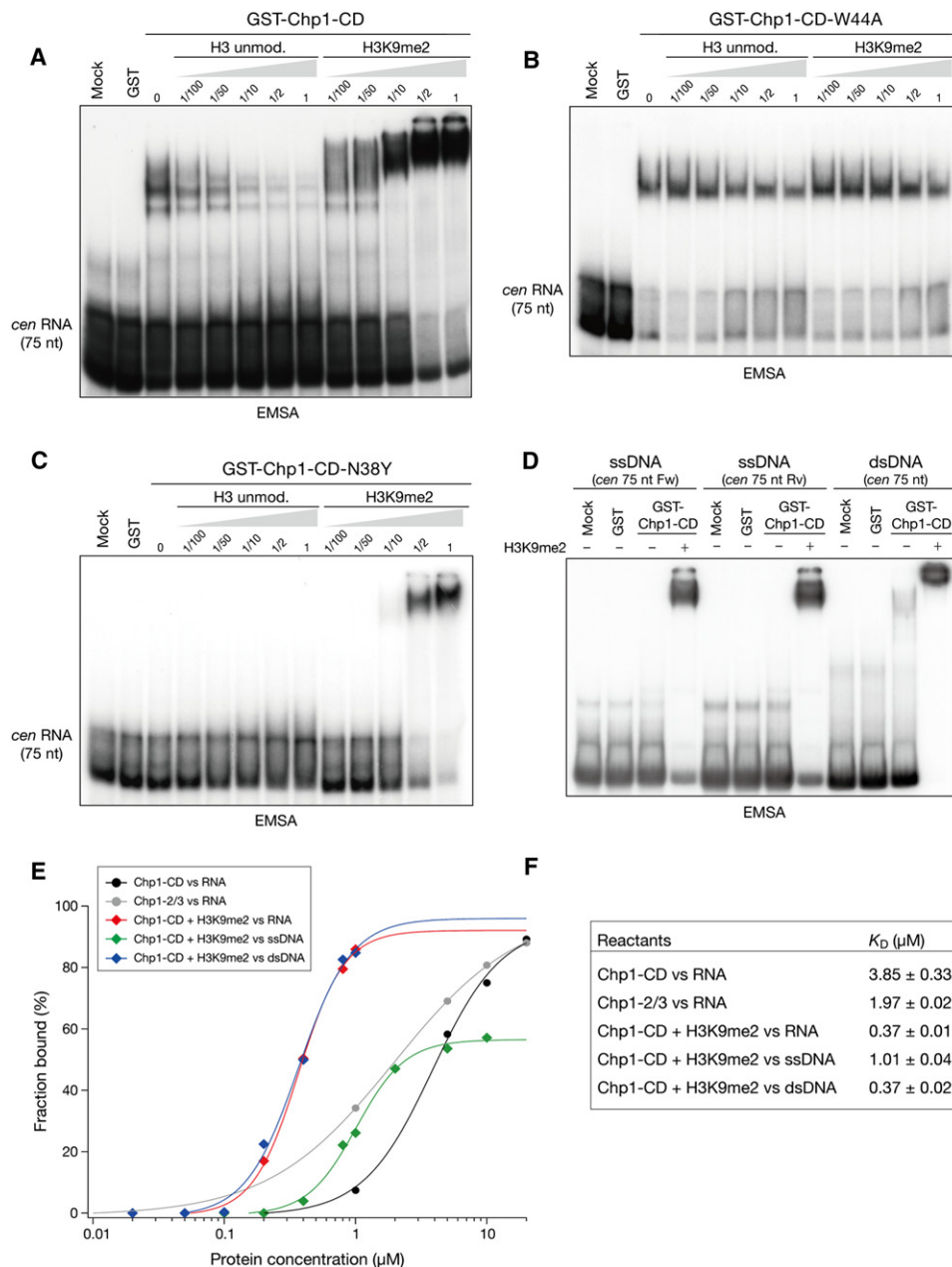


**Figure 3. H3K9me Changes the Nucleic Acid-Binding Activity of the Chp1-CD**

(A–C) EMSA using GST-fused wild-type Chp1-CD (A), Chp1-CD-W44A (B), or Chp1-CD-N38Y (C). Each CD protein (50 pmol) was incubated with  $^{32}$ P-labeled, *cen-dh* single-stranded RNA (ssRNA) (75 nt) in the presence or absence of the indicated molar masses (0.5–50 pmol) of unmodified or K9-dimethylated histone H3 (H3K9me2) peptide (1–20 aa).

(D) EMSA using GST-fused wild-type Chp1-CD and various DNA probes. Chp1-CD protein (50 pmol) was examined in the presence or absence of an equal molar mass of H3K9me2 peptide.

(E) Binding isotherm; the ratios of the bound nucleic acid probes determined by titration EMSAs (Figure S3) are plotted against the concentrations of the free or H3K9me2-bound GST-Chp1-CD or GST-Chp1-2/3. The data were fit to the Hill equation to yield the apparent dissociation constants.

(F) The dissociation constants measured by titration EMSAs.

### Chp1-CD RNA- and DNA-Binding Is Required for Chp1's Silencing Function

To investigate the role of nucleic acid binding in Chp1 function in vivo, the above mutant Chp1 proteins were expressed from the endogenous *chp1*<sup>+</sup> locus, and their effects on centro-

meric *otr1R::ura4*<sup>+</sup> silencing was examined (Figure 5A) together with their centromeric association (Figures 6A and S6A). Immunoblotting assays showed that the Chp1 mutant protein levels were comparable to, or slightly higher than, that of wild-type Chp1 (Figure S5).



**Table 1. Structural Statistics of the Chp1-CD/H3K9me3 and Swi6-CD**

	Chp1-CD/H3K9me3	Swi6-CD
Total distance restraints	866	746
Short range ( $ i-j  \leq 1$ )	473	443
Medium range ( $1 <  i-j  < 5$ )	99	101
Long range ( $ i-j  \geq 5$ )	294	202
Hydrogen bonds	22	12
NOEs between protein and peptide	116	–
Dihedral angle restraints <sup>a</sup>		
$\Phi$	50	48
$\Psi$	50	48
Maximum and total constraint violations		
Upper distance limits (Å)	0.0051 ± 0.0005 / 0.13 ± 0.02	0.0034 ± 0.0005 / 0.11 ± 0.01
Lower distance limits (Å)	0.0009 ± 0.0008	0.0004 ± 0.0006
van der Waals contacts (Å)	0.15 ± 0.04 / 3.2 ± 0.2	0.10 ± 0.03 / 1.5 ± 0.2
Torsion angle ranges (°)	0.5428 ± 0.0611 / 2.96 ± 0.26	0.3915 ± 0.0819 / 2.02 ± 0.53
Average CYANA target function (Å <sup>2</sup> ) <sup>b</sup>	0.50 ± 0.0544	0.20 ± 0.0293
Restraints statistics <sup>c</sup>		
NOE violations > 0.5 Å	0	–
Dihedral violations > 5°	0	–
CNS energies (Kcal/mol) <sup>c</sup>		
$E_{\text{total}}$	–3822.9 ± 79.8	–
$E_{\text{vdw}}$	–230.4 ± 12.4	–
$E_{\text{elec}}$	–4455.9 ± 83.4	–
Average pairwise rmsd <sup>d,e</sup>		
Backbone atoms (Å)	0.63 ± 0.14	0.56 ± 0.08
Heavy atoms (Å)	1.58 ± 0.24	1.11 ± 0.10
Ramachandran plot statistics <sup>d,e,f</sup>		
Residues in most favored regions (%)	88.7	90.3
Residues in additional allowed regions (%)	11.3	9.7

<sup>a</sup>Generated from program TALOS+.<sup>b</sup>Values for ensemble of the 20 lowest structures out of 600 calculated.<sup>c</sup>The statistics are obtained from an ensemble of 20 lowest-energy water-refined structures.<sup>d</sup>The Chp1-CD residues 17–73.<sup>e</sup>The Swi6-CD residues 82–134.<sup>f</sup>As determined by the program PROCHECK-NMR.

(Figure 5A) and a decrease in the centromeric association of mutant Chp1 (Figure 6B). This indicated that the nucleic acid-binding activity associated with H3K9me-bound Chp1-CD is required for proper targeting of Chp1 and its silencing function.

While the phenotype of  $\alpha\text{mut1}$  mutant cells was similar to that of W44A cells with regard to *otr1R::ura4<sup>+</sup>* expression (Figure 5A), the phenotype of  $\alpha\text{mut1}$  cells was more severe than that of W44A in 5-fluoroorotic acid (FOA)-containing medium, implying that the mechanisms underlying these silencing defects were

different. Although there was little or no observable heterochromatic association for Chp1-W44A (Figure 6A), the silencing defect of the Chp1-W44A cells was clearly milder than that of  $\Delta\text{chp1}$  cells (Figure 5A, see FOA-resistant colonies). Given that the W44A mutation abolished Chp1-CD's H3K9me-binding ability (Figures 2E and S2D), Chp1 probably retained partial silencing function independently of H3K9me. To examine whether free Chp1-CD's RNA-binding activity was involved with this partial functionality, we combined the W44A mutation with the N38Y or WY/DPS amino acid substitutions and examined the silencing function of the resulting mutant Chp1 proteins (Chp1-W44A,N38Y and Chp1-W44A,WY/DPS). The silencing defect was more severe in cells expressing these Chp1 mutants than in the original Chp1-W44A cells (Figure 5B). The fact that the combined mutations show enhanced growth on –Ura plates and increase in *ura4<sup>+</sup>* transcript levels compared to that of the single W44A mutant is consistent with a role for the Chp1CD RNA-binding activity in centromeric silencing. A similar additive effect was observed by replacing the C-terminal basic residues of Chp1-CD with those of Swi6-CD (Figure 5B, W44A, $\alpha\text{mut1}$ ), which also abolished the free Chp1-CD's ability to bind RNA (Figure 4F). Together, these results suggested that Chp1 can repress centromeric transcripts without forming a stable interaction with H3K9me and that free Chp1-CD's RNA-binding ability also plays a role in its silencing function.

### CD and RRM Cooperate to Repress Centromeric Transcripts

Although cells expressing Chp1 $\Delta$ CD had clear silencing defects, their *otr1R::ura4<sup>+</sup>* expression levels differed from those found in *chp1*-deleted cells (Figures 5B and 5C). Since Chp1 might bind to RNA via its central RRM, we next examined whether the RRM might be involved in the remaining silencing function of Chp1 $\Delta$ CD. Deleting the central RRM did not noticeably affect centromeric silencing (Figure 5C); however, deleting the RRM and the CD had an additive effect (Figure 5C). Importantly, the *otr1R::ura4<sup>+</sup>* derepression state of cells expressing Chp1 $\Delta$ CD $\Delta$ RRM was comparable to that of the  $\Delta\text{chp1}$  null cells. These results suggested that CD and RRM act cooperatively, at least in Chp1's silencing function when performed without being stably bound to H3K9me.

RNA immunoprecipitation (RNA-IP) experiments have shown an association between Chp1 and noncoding centromeric transcripts (Motamedi et al., 2004, 2008). To directly test whether CD or RRM is responsible for forming an association with centromeric transcripts, we conducted an RNA-IP assay for wild-type and mutant Chp1. As previously noted, the centromeric (*cen dh*) RNA was clearly enriched in the FLAG-Chp1-WT precipitate, whereas it was only negligibly enriched in that of the untagged control or  $\Delta\text{chp1}$  strains or when reverse transcription was absent (Figure 6G). The N38Y and WY/DPS precipitates were also highly enriched in *cen dh* RNA, although a slight reduction of enrichment was observed for N38Y precipitates. This was consistent with these Chp1 mutants showing silencing ability comparable to that of wild-type Chp1 (Figure 5A) and associating stably with centromeric repeats (Figure 6A).

Strikingly, the centromeric *dh* transcript levels were greatly reduced in the precipitates of W44A,  $\alpha\text{mut1}$ , or  $\Delta$ CD (Figure 6G),

Molecular Cell

Chp1 CD links RNA and K9-Methylated Histone H3

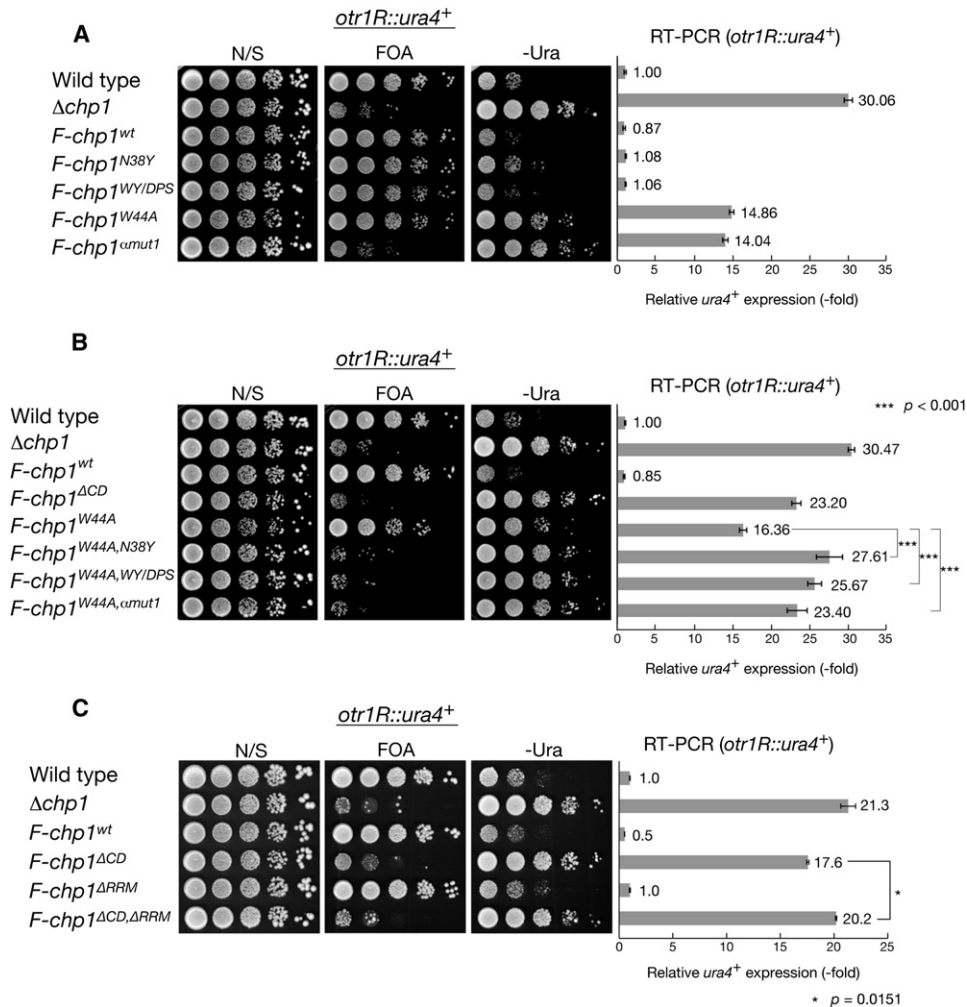


**Figure 5. Intrinsic Nucleic Acid-Binding Activities of Chp1-CD Are Required for Heterochromatic Silencing**

(A–C) FLAG-tagged, wild-type and mutant Chp1 proteins were produced from the original *chp1*<sup>+</sup> locus. Spotting assays for *otr1R::ura4*<sup>+</sup> silencing are shown at left; the  $\Delta$ *chp1* strain was used as a negative control. A serially diluted culture of each indicated strain was spotted onto nonselective medium (N/S), medium containing 5FOA (FOA), or medium lacking uracil (–Ura) (left). Expression levels of the *ura4*<sup>+</sup> silencing reporter were evaluated by qRT-PCR analyses (right). Averages and standard deviations are shown of at least three independent biological repeats.

although they retained RRM, indicating that both the Chp1-CD H3K9me-binding and intrinsic nucleic acid-binding activities are required for Chp1’s efficient association with centromeric transcripts. Although these mutant Chp1 proteins appeared to retain partial silencing function via their intrinsic RNA-binding activity (Figures 5B and 5C), their centromeric transcript enrichment levels were comparable to those of control  $\Delta$ *chp1* cells (Figure 6G). Direct associations between Chp1 and centromeric transcript RNA at a site distant from chromatin might be difficult to detect with this RNA-IP assay, since the assay relies on protein-protein crosslinking formed by formaldehyde.

Considering that the centromeric *dh* transcript levels were greatly reduced in the precipitates of  $\Delta$ CD, it was likely that the central RRM plays a minor role in associating Chp1 with centromeric transcripts. However, centromeric *dh* RNA enrichment was also clearly reduced in the  $\Delta$ RRM precipitates. This was

surprising, because cells expressing Chp1 $\Delta$ RRM showed wild-type silencing levels (Figure 6A) and Chp1 $\Delta$ RRM robustly associated with centromeric chromatin (Figure 6C). These results suggested that although the RRM is required for Chp1 to associate efficiently with centromeric transcripts, H3K9me binding via the CD might play a dominant role in maintaining centromeric silencing.

**H3K9me-Bound Clr4-CD Also Binds RNA and DNA**

In the initial RNA EMSA, Chp2-CD, Swi6-CD, and Clr4-CD failed to bind *cen* RNA (Figure 1H). However, the above results for Chp1-CD raised the possibility that these CDs might be able to bind RNA or DNA when also bound to target histone tails. To test this possibility, unmodified or H3K9me2 peptide was added to RNA EMSAs for Clr4-CD, Swi6-CD, and Chp2-CD. Notably, the addition of H3K9me2 peptide conferred an RNA-binding ability to Clr4-CD (Figure 7A), but it did not produce any

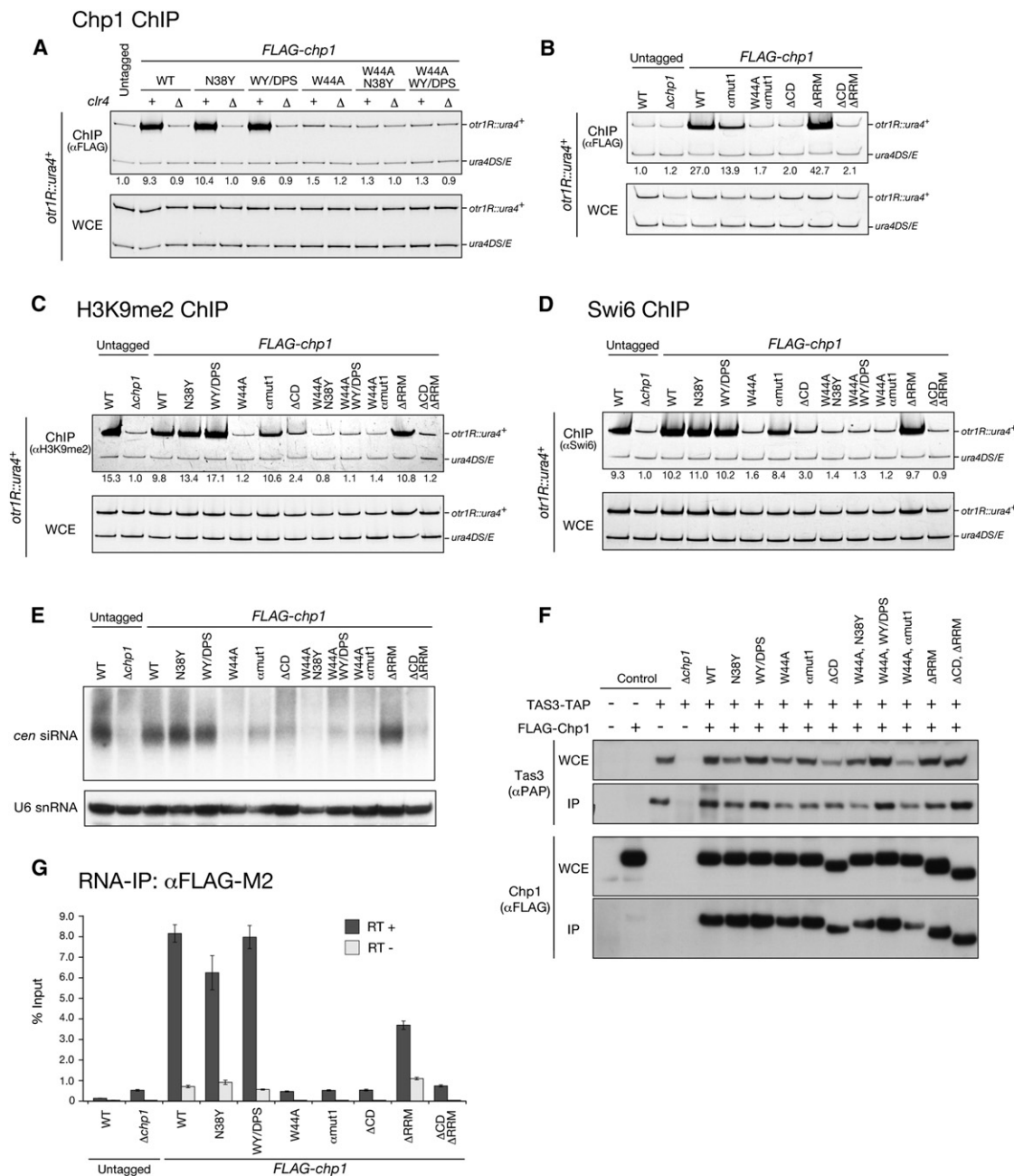


**Figure 6. Intrinsic Nucleic Acid-Binding Activities of Chp1-CD Are Required for Heterochromatin Assembly**

(A–D) Chromatin immunoprecipitation (ChIP) assays showing Chp1 (A and B), H3K9me2 (C), and Swi6 (D) levels at centromeric *otr1R::ura4<sup>+</sup>* regions. Wild-type cells without tagged Chp1 and  $\Delta chp1$  cells were used as controls. The *otr1R::ura4<sup>+</sup>* signal enrichment relative to the *ura4DS/E* signal enrichment in the ChIP results were normalized to the whole-cell extract (WCE) signals, and are shown beneath each lane.

(E) Northern-blot analysis of centromeric siRNAs prepared from indicated strains. Loading control: U6 snRNA.

(F) The RITS complex in each indicated strain was purified by Tas3-TAP. Tas3-TAP and Chp1 proteins in precipitates were detected by western analysis using  $\alpha$ FLAG-M2 and  $\alpha$ PAP antibodies.

(G) RNA immunoprecipitation (RNA-IP) experiments using strains expressing wild-type or mutant Chp1. RNAs isolated from the  $\alpha$ FLAG M2-immunoprecipitated fractions were subjected to qRT-PCR analysis using primers for the *cen-dh* transcript. PCR results of mock reactions without reverse transcription are also shown. Averages and standard deviations are shown of at least three independent biological repeats.

observable change for Swi6- or Chp2-CD (Figure 7B and data not shown). In addition, Clr4-CD efficiently bound ssDNA and dsDNA when bound to H3K9me2 (Figure S7A). These results

suggested that the nucleic acid-binding ability is associated with a subset of CDs, and this difference may relate to the distinct functions of the CD proteins.

Like Chp1-CD, Clr4-CD has a block of basic amino acid residues in its C-terminal  $\alpha$ -helix region (Figure 2A). To examine whether these basic residues (K58–R62) were involved in Clr4-CD's RNA binding, they were replaced with residues corresponding to Swi6-CD, and the mutant Clr4-CD ( $\alpha$ mut) was subjected to the RNA EMSA (Figures 7C, S7B, and S7C). Wild-type Clr4-CD bound RNA in the presence of H3K9me2 peptide (Figures 7A and 7C). This RNA binding was abolished in the  $\alpha$ mut, suggesting that the C-terminal  $\alpha$ -helix basic residues are essential for Clr4-CD's nucleic acid binding.

To examine whether Clr4-CD's RNA-binding activity is involved in Clr4 function in vivo, we expressed mutant Clr4 from the endogenous *clr4*<sup>+</sup> locus and examined its effect on centromeric *otr1R::ura4*<sup>+</sup> silencing. Immunoblotting assays showed that the mutant Clr4 protein levels were comparable to those of wild-type Clr4 (Figure S7D). Although the effect was milder than that seen in  $\Delta$ *clr4* cells, this mutation caused enhanced growth on –Ura plates (Figure 7D), suggesting that Clr4-CD's C-terminal  $\alpha$ -helix basic residues contribute to Clr4's silencing function and that Clr4-CD's RNA-binding activity might also be involved in its chromatin targeting.

To investigate the role of nucleic acid-binding activity in the distinct function of CD proteins, a domain swapping experiment was performed, by replacing the Swi6-CD with each of other CDs (Figures 7E, S7E, and S7F). Mutant cells expressing chimeric Swi6 containing Chp2-CD showed similar silencing function to that of cells expressing wild-type Swi6. In contrast, mutant cells expressing Swi6 with either Chp1-CD or Clr4-CD exhibited a failure to support silencing function (Figure 7E). These results suggested that the CD does not merely function to interact with H3K9me but directly provides a division of roles for CD proteins.

## DISCUSSION

The chromodomain (CD) is a highly conserved protein module that is critical for targeting proteins to their action sites in chromatin. CD's best-known role is in binding to methylated histone tails. However, the mechanisms behind CD's various functions remain unclear. The present study demonstrates that Chp1-CD's intrinsic nucleic acid-binding activity is required for heterochromatin gene silencing in fission yeast.

In contrast to the three other H3K9me-recognizing *S. pombe* CDs, Chp1-CD can bind RNA even in the absence of H3K9me. This RNA-binding activity is likely to facilitate the targeting of RNA for silencing through the RNAi pathway. Indeed, mutations of the residues critical for free Chp1-CD's binding of RNA added to the silencing defect in the Chp1-W44A mutant, which is deficient in H3K9me binding (Figure 5B). Given that heterochromatin requires dynamic remodeling during the cell cycle (Chen et al., 2008; Kloc et al., 2008), this RNA-binding ability may act as a back-up system to reinforce the targeting of nascent transcripts. We also demonstrated that Chp1's central RRM cooperates with its CD to silence centromeric transcripts. These results suggest that the targeting of nascent transcripts by the RITS complex is achieved by multiple interactions involving Chp1-CD and RRM, and by the base-pairing of Ago1-bound siRNAs. As demonstrated by our titration EMSAs, the RNA-binding affinity of free Chp1-CD is, however, apparently weaker than

that induced by binding to H3K9me2. In addition, H3K9me-bound Chp1-CD shows a comparable binding affinity for dsDNA. Thus, intrinsic nucleic-binding activity of Chp1-CD may act primarily to stably bind to H3K9me-enriched chromatin.

The critical residues for free Chp1-CD's nucleic acid binding were determined by candidate mutational analyses (Figure 2). However, the structural mechanisms by which Chp1 binds RNA remain unclear. Our NMR data suggest that the region including W49 and Y50 does not have a fixed structure and that N38's direct association with RNA was not observed in titration analyses (Figures S4A and S4C). Considering that mutant Chp1-CDs deficient in H3K9me binding bound RNA more strongly than did wild-type Chp1-CD (Figure 2D), free Chp1-CD's binding of RNA is linked with its structural flexibility, which might be decreased by N38Y and WY/DPS mutations, but conversely increased by W44A and other mutations.

H3K9me-bound Chp1-CD can also bind RNA and DNA via a block of basic residues in its C-terminal  $\alpha$ -helix. While structural information is limited, the manner of this binding appears to be similar in Clr4-CD and Chp1-CD (Figures 7A and 7C). Mutation analyses demonstrated that these nucleic acid-binding activities are required for centromeric silencing (Figures 5A and 7D). Given that the histone tails and DNA wrapped around core histones are located close to one another, nucleosomal or linker DNA may be a substrate of H3K9me-bound Chp1-CD to enhance its chromatin association. Alternatively, these activities may serve to tether nascent transcripts to H3K9me-enriched chromatin. A recent report showed that a mouse Pc protein, Cbx7-CD, can bind to RNA (Bernstein et al., 2006) and that this activity contributes to Cbx7's function in regulating cellular senescence (Yap et al., 2010). Although the site responsible for RNA binding for Cbx7-CD is distinct from that of Chp1-CD (Figures 4A and 4B), it is possible that the coordinated methylated histone-binding, DNA-binding, and RNA-binding activities function similarly to establish higher-order chromatin in different species of fission yeast and mammals.

A previous report showed that Chp1-CD has a higher affinity than Swi6-CD for H3K9me (Schalch et al., 2009). On the other hand, it has been proposed that the acetyl modification of H3K4 (H3K4ac) switches the H3K9me-binding protein from Chp1/Clr4 to Chp2/Swi6 (Xhemalce and Kouzarides, 2010). The present study strongly suggests that CD proteins' intrinsic nucleic acid-binding activities are also critical properties supporting the distinct functions of each CD (Figure 7E). Considering that no intrinsic nucleic acid-binding activity was detected for Swi6-CD or Chp2-CD, it appears to be attributable that this activity is required for the initial establishment step, but is dispensable for further maintaining processes. Since nucleic acid-binding activity has been linked with the CD proteins of diverse species (Akhtar et al., 2000; Bernstein et al., 2006; Shimojo et al., 2008; Yap et al., 2010), this property may also contribute to the distinct CD-protein functions in other biological processes.

## EXPERIMENTAL PROCEDURES

### Strains and Plasmids

To obtain strains expressing mutant Chp1, a portion of the *chp1*<sup>+</sup>-coding region (–542 to +1722) was cloned into pBluescript with an *ura4*<sup>+</sup> marker

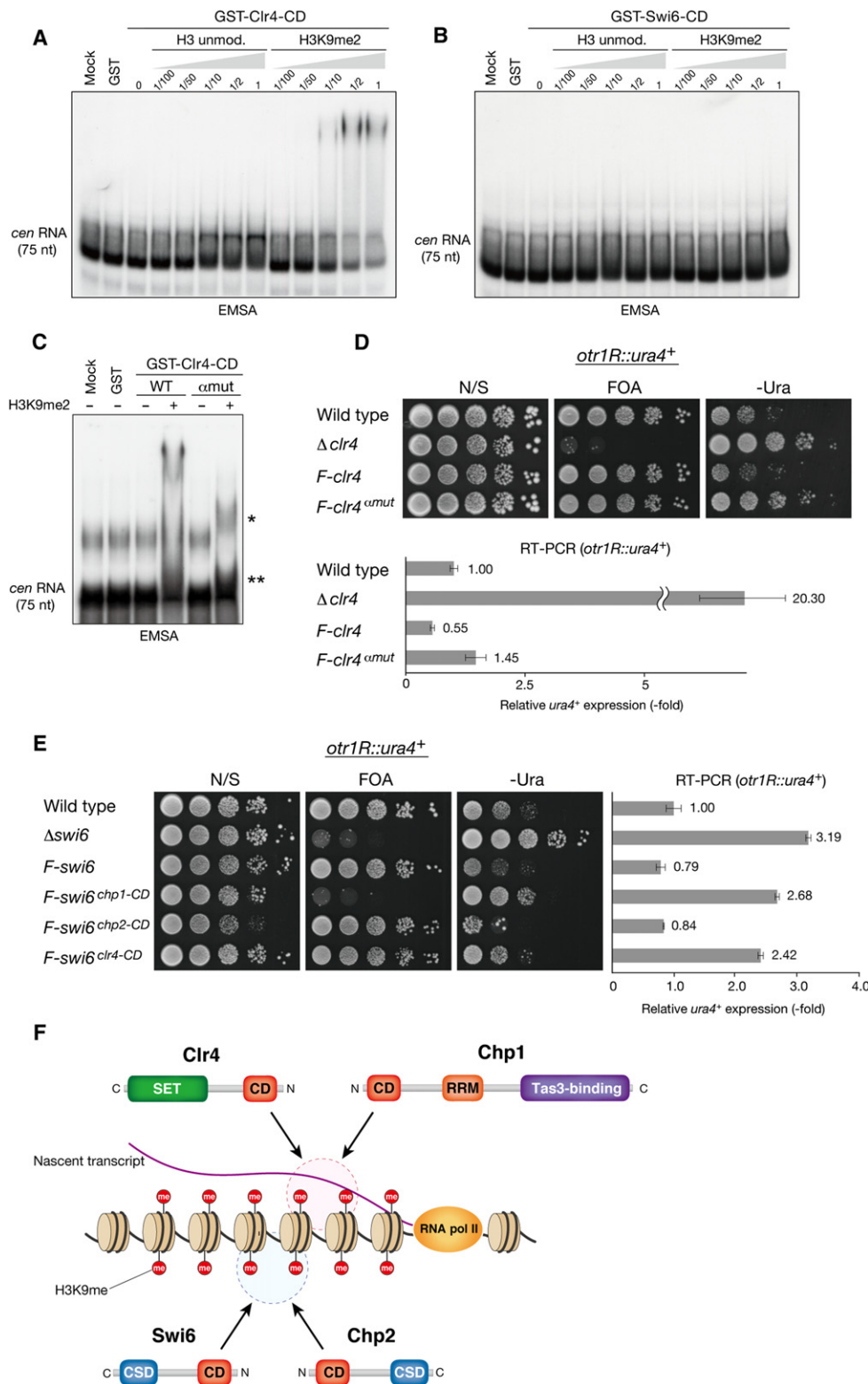


**Figure 7. The Nucleic Acid-Binding Activity of Each CD Protein Contributes to its Distinct Function**

(A and B) EMSAs using GST-fused Clr4-CD (A) or Swi6-CD (B). Each CD protein (50 pmol) was examined as described in Figure 3.

(C) RNA EMSAs of wild-type and mutant Clr4-CDs. Wild-type (WT) and mutant ( $\alpha$ mut) Clr4-CDs were examined in the presence (+) or absence (-) of an equimolar amount of H3K9me2 peptide (1–20 aa). Asterisks indicate band shift induced by adding H3K9me2 peptide.

## Molecular Cell

### Chp1 CD links RNA and K9-Methylated Histone H3

gene. Site-directed mutagenesis was used to introduce a BamHI restriction site immediately after the ATG codon, and the DNA fragment for a 3xFLAG epitope was inserted in the BamHI site. Each mutation or deletion was introduced by site-directed mutagenesis. The resultant plasmids were cleaved by BglII and introduced into the original *chp1<sup>+</sup>* locus. To replace the wild-type *chp1<sup>+</sup>* allele with the mutant *chp1* allele, strains that had lost the *ura4<sup>+</sup>* gene through internal homologous recombination were isolated using counter-selective medium containing FOA. Strains harboring *otr1R::ura4<sup>+</sup>* were constructed using standard genetic crosses. For other details, see [Supplemental Experimental Procedures](#).

#### Antibodies

The following antibodies were used: peroxidase-conjugated anti-FLAG M2 (A8592; Sigma), anti-FLAG M2 affinity gel (Sigma), anti-TAT1 (kindly provided by K. Gull, University of Oxford), and anti-H3K9me2 (Sadaie et al., 2004). Anti-GST rabbit polyclonal antibodies were raised against recombinant GST. Antiserum was loaded into a column crosslinked with GST to obtain the antibodies.

#### RNA EMSAs

RNA EMSAs were performed as described previously (Bernstein et al., 2006; Iida et al., 2006) with some modifications. For details, see [Supplemental Experimental Procedures](#).

#### Silencing Assays and Reverse Transcription-PCR Analyses

Silencing assays and reverse transcription-PCR (RT-PCR) analyses were performed as described previously (Sadaie et al., 2008).

#### Chromatin Immunoprecipitation

Chromatin immunoprecipitation (ChIP) analysis was performed as described previously (Sadaie et al., 2004, 2008). FLAG-tagged proteins were immunoprecipitated using anti-FLAG M2 affinity gel (Sigma). PCR products were separated and analyzed on 10% polyacrylamide gels (ATTO).

#### ACCESSION NUMBERS

Protein Data Bank accession codes for the Chp1-CD/H3K9me3 complex and the free Swi6-CD structures are 2RSN and 2RSO, respectively.

#### SUPPLEMENTAL INFORMATION

Supplemental Information includes seven figures, two tables, Supplemental Experimental Procedures, and Supplemental References and can be found with this article online at doi:10.1016/j.molcel.2012.05.017.

#### ACKNOWLEDGMENTS

We thank J. Partridge for the GST-Chp1CD plasmid, K. Gull for the TAT1 antibody, and T. Kajitani for the RIP protocol. We also thank K. H. Hamada and D. Goto for critical reading of the manuscript, members of the Nakayama Lab for helpful discussions, and S. Seno for excellent secretarial work. This research was supported by a Grant-in-Aid from the Ministry of Education, Culture, Sports, Science, and Technology of Japan.

Received: November 7, 2011

Revised: March 26, 2012

Accepted: April 26, 2012

Published online: June 21, 2012

#### REFERENCES

- Akhtar, A., Zink, D., and Becker, P.B. (2000). Chromodomains are protein-RNA interaction modules. *Nature* 407, 405–409.
- Allshire, R.C., Nimmo, E.R., Ekwall, K., Javerzat, J.P., and Cranston, G. (1995). Mutations derepressing silent centromeric domains in fission yeast disrupt chromosome segregation. *Genes Dev.* 9, 218–233.
- Bannister, A.J., Zegerman, P., Partridge, J.F., Miska, E.A., Thomas, J.O., Allshire, R.C., and Kouzarides, T. (2001). Selective recognition of methylated lysine 9 on histone H3 by the HP1 chromo domain. *Nature* 410, 120–124.
- Bernstein, E., Duncan, E.M., Masui, O., Gil, J., Heard, E., and Allis, C.D. (2006). Mouse polycomb proteins bind differentially to methylated histone H3 and RNA and are enriched in facultative heterochromatin. *Mol. Cell. Biol.* 26, 2560–2569.
- Bouazoune, K., Mitterweger, A., Längst, G., Imhof, A., Akhtar, A., Becker, P.B., and Brehm, A. (2002). The dMi-2 chromodomains are DNA binding modules important for ATP-dependent nucleosome mobilization. *EMBO J.* 21, 2430–2440.
- Bühler, M., and Moazed, D. (2007). Transcription and RNAi in heterochromatic gene silencing. *Nat. Struct. Mol. Biol.* 14, 1041–1048.
- Bühler, M., Verdel, A., and Moazed, D. (2006). Tethering RITS to a nascent transcript initiates RNAi- and heterochromatin-dependent gene silencing. *Cell* 125, 873–886.
- Buker, S.M., Iida, T., Bühler, M., Villén, J., Gygi, S.P., Nakayama, J., and Moazed, D. (2007). Two different Argonaute complexes are required for siRNA generation and heterochromatin assembly in fission yeast. *Nat. Struct. Mol. Biol.* 14, 200–207.
- Chen, E.S., Zhang, K., Nicolas, E., Cam, H.P., Zofall, M., and Grewal, S.I. (2008). Cell cycle control of centromeric repeat transcription and heterochromatin assembly. *Nature* 451, 734–737.
- Djupedal, I., Kos-Braun, I.C., Mosher, R.A., Söderholm, N., Simmer, F., Hardcastle, T.J., Fender, A., Heidrich, N., Kagansky, A., Bayne, E., et al. (2009). Analysis of small RNA in fission yeast; centromeric siRNAs are potentially generated through a structured RNA. *EMBO J.* 28, 3832–3844.
- Fischer, T., Cui, B., Dhakshnamoorthy, J., Zhou, M., Rubin, C., Zofall, M., Veenstra, T.D., and Grewal, S.I. (2009). Diverse roles of HP1 proteins in heterochromatin assembly and functions in fission yeast. *Proc. Natl. Acad. Sci. USA* 106, 8998–9003.
- Grewal, S.I., and Jia, S. (2007). Heterochromatin revisited. *Nat. Rev. Genet.* 8, 35–46.
- Iida, T., Kawaguchi, R., and Nakayama, J. (2006). Conserved ribonuclease, Eri1, negatively regulates heterochromatin assembly in fission yeast. *Curr. Biol.* 16, 1459–1464.
- Jacobs, S.A., and Khorasanizadeh, S. (2002). Structure of HP1 chromodomain bound to a lysine 9-methylated histone H3 tail. *Science* 295, 2080–2083.
- Kloc, A., Zaratiegui, M., Nora, E., and Martienssen, R. (2008). RNA interference guides histone modification during the S phase of chromosomal replication. *Curr. Biol.* 18, 490–495.
- Lachner, M., O'Carroll, D., Rea, S., Mechtler, K., and Jenuwein, T. (2001). Methylation of histone H3 lysine 9 creates a binding site for HP1 proteins. *Nature* 410, 116–120.
- Motamedi, M.R., Verdel, A., Colmenares, S.U., Gerber, S.A., Gygi, S.P., and Moazed, D. (2004). Two RNAi complexes, RITS and RDRC, physically interact and localize to noncoding centromeric RNAs. *Cell* 119, 789–802.
- Motamedi, M.R., Hong, E.J., Li, X., Gerber, S., Denison, C., Gygi, S., and Moazed, D. (2008). HP1 proteins form distinct complexes and mediate

(D) FLAG-tagged wild-type or mutant Ctr4 was expressed from the original *ctr4<sup>+</sup>* locus; spotting assays (upper) and qRT-PCR analyses (lower) of the *otr1R::ura4<sup>+</sup>* silencing state are shown.

(E) FLAG-tagged wild-type or CD-swapped Swi6 was expressed from original *swi6<sup>+</sup>* locus. The silencing state of *otr1R::ura4<sup>+</sup>* was assayed by the spotting assays (left), and evaluated by qRT-PCR analysis (right). Averages and standard deviations are shown of at least two independent biological repeats (D and E).

(F) Proposed model for the role of CD protein's intrinsic RNA binding in heterochromatin assembly. See text for details.

- heterochromatic gene silencing by nonoverlapping mechanisms. *Mol. Cell* **32**, 778–790.
- Nakayama, J., Rice, J.C., Strahl, B.D., Allis, C.D., and Grewal, S.I. (2001). Role of histone H3 lysine 9 methylation in epigenetic control of heterochromatin assembly. *Science* **292**, 110–113.
- Noma, K., Sugiyama, T., Cam, H., Verdel, A., Zofall, M., Jia, S., Moazed, D., and Grewal, S.I. (2004). RITS acts in cis to promote RNA interference-mediated transcriptional and post-transcriptional silencing. *Nat. Genet.* **36**, 1174–1180.
- Paro, R., and Hogness, D.S. (1991). The Polycomb protein shares a homologous domain with a heterochromatin-associated protein of *Drosophila*. *Proc. Natl. Acad. Sci. USA* **88**, 263–267.
- Partridge, J.F., Scott, K.S., Bannister, A.J., Kouzarides, T., and Allshire, R.C. (2002). cis-acting DNA from fission yeast centromeres mediates histone H3 methylation and recruitment of silencing factors and cohesin to an ectopic site. *Curr. Biol.* **12**, 1652–1660.
- Partridge, J.F., DeBeauchamp, J.L., Kosinski, A.M., Ulrich, D.L., Hadler, M.J., and Noffsinger, V.J. (2007). Functional separation of the requirements for establishment and maintenance of centromeric heterochromatin. *Mol. Cell* **26**, 593–602.
- Petrie, V.J., Wuitschick, J.D., Givens, C.D., Kosinski, A.M., and Partridge, J.F. (2005). RNA interference (RNAi)-dependent and RNAi-independent association of the Chp1 chromodomain protein with distinct heterochromatic loci in fission yeast. *Mol. Cell. Biol.* **25**, 2331–2346.
- Sadaie, M., Iida, T., Urano, T., and Nakayama, J. (2004). A chromodomain protein, Chp1, is required for the establishment of heterochromatin in fission yeast. *EMBO J.* **23**, 3825–3835.
- Sadaie, M., Kawaguchi, R., Ohtani, Y., Arisaka, F., Tanaka, K., Shirahige, K., and Nakayama, J. (2008). Balance between distinct HP1 family proteins controls heterochromatin assembly in fission yeast. *Mol. Cell. Biol.* **28**, 6973–6988.
- Schalch, T., Job, G., Noffsinger, V.J., Shanker, S., Kuscu, C., Joshua-Tor, L., and Partridge, J.F. (2009). High-affinity binding of Chp1 chromodomain to K9 methylated histone H3 is required to establish centromeric heterochromatin. *Mol. Cell* **34**, 36–46.
- Shanker, S., Job, G., George, O.L., Creamer, K.M., Shaban, A., and Partridge, J.F. (2010). Continuous requirement for the Clr4 complex but not RNAi for centromeric heterochromatin assembly in fission yeast harboring a disrupted RITS complex. *PLoS Genet.* **6**, e1001174.
- Shimojo, H., Sano, N., Moriwaki, Y., Okuda, M., Horikoshi, M., and Nishimura, Y. (2008). Novel structural and functional mode of a knot essential for RNA binding activity of the Esa1 presumed chromodomain. *J. Mol. Biol.* **378**, 987–1001.
- Sugiyama, T., Cam, H., Verdel, A., Moazed, D., and Grewal, S.I. (2005). RNA-dependent RNA polymerase is an essential component of a self-enforcing loop coupling heterochromatin assembly to siRNA production. *Proc. Natl. Acad. Sci. USA* **102**, 152–157.
- Verdel, A., Jia, S., Gerber, S., Sugiyama, T., Gygi, S., Grewal, S.I., and Moazed, D. (2004). RNAi-mediated targeting of heterochromatin by the RITS complex. *Science* **303**, 672–676.
- Volpe, T.A., Kidner, C., Hall, I.M., Teng, G., Grewal, S.I., and Martienssen, R.A. (2002). Regulation of heterochromatic silencing and histone H3 lysine-9 methylation by RNAi. *Science* **297**, 1833–1837.
- Xhemalce, B., and Kouzarides, T. (2010). A chromodomain switch mediated by histone H3 Lys 4 acetylation regulates heterochromatin assembly. *Genes Dev.* **24**, 647–652.
- Yap, K.L., Li, S., Muñoz-Cabello, A.M., Raguz, S., Zeng, L., Mujtaba, S., Gil, J., Walsh, M.J., and Zhou, M.M. (2010). Molecular interplay of the noncoding RNA ANRIL and methylated histone H3 lysine 27 by polycomb CBX7 in transcriptional silencing of INK4a. *Mol. Cell* **38**, 662–674.
- Zhang, K., Mosch, K., Fischle, W., and Grewal, S.I. (2008). Roles of the Clr4 methyltransferase complex in nucleation, spreading and maintenance of heterochromatin. *Nat. Struct. Mol. Biol.* **15**, 381–388.